

# Structural and luminescent properties of Fe<sup>3+</sup> doped tin oxide thin films by spray pyrolysis

M. C. RAO<sup>a,\*</sup>, K. RAVINDRANADH<sup>b</sup>, T. SATYANARAYANA<sup>c</sup>, G. NAGARJUNA<sup>d</sup>, R. K. N. R. MANEPALLI<sup>e</sup>

<sup>a</sup>Department of Physics, Andhra Loyola College, Vijayawada - 520 008, India

<sup>b</sup>Physics Division, Department of Basic Sciences & Humanities, Chirala Engineering College, Chirala-523 157, India

<sup>c</sup>Department of EIE, Lakireddy Bali Reddy College of Engineering, Mylavaram- 521230, India

<sup>d</sup>Department of Chemistry, S. R. R. & C. V. R. Govt. College, Vijayawada-520 004, India

<sup>e</sup>Department of Physics, The Hindu College, Krishna University, Machilipatnam-521001, India

The study and application of thin film technology is entirely entered in to almost all the branches of science and technology. Semiconductor oxide thin films are materials with numerous applications in electronic and optoelectronic devices as well as some other applications such as protective coatings, heat mirrors and catalysis. Transparent conducting oxide films have been widely used in the fields of flat panel displays, solar cells, touch panels and other optoelectronic devices owing to their high electrical conductivity and optical transmittance in visible region. Fe<sup>3+</sup> doped tin oxide thin films were prepared by chemical spray pyrolysis synthesis and characterized by different spectroscopic techniques. The morphologies of prepared sample were analyzed by using SEM and TEM studies. Functional groups of the prepared sample were observed in the FT-IR spectrum. PL studies of Fe<sup>3+</sup> doped SnO<sub>2</sub> thin films exhibit ultraviolet and blue emission bands. CIE chromaticity coordinates were also calculated from emission spectrum of Fe<sup>3+</sup> doped SnO<sub>2</sub> thin films.

(Received October 21, 2015; accepted April 6, 2017)

**Keywords:** SnO<sub>2</sub>, Thin films, Spray pyrolysis, SEM, TEM, FT-IR and Photoluminescence

## 1. Introduction

The interest in the surface structures with their special properties has increased considerably due to extensive applications in micro and optoelectronics. It is known that the properties of films of submicron size can be different from those of structures having macroscopic dimensions [1]. The parameters that change the properties of films are the thickness, number of layers, uniformity of the films, size of clusters and nanocrystals [2]. The presence of small particles and nano-sized elements leads to changes in material properties such as electrical conductivity, refractive index, band gap, magnetic properties, strength and others [3-5]. Metal oxides play a very important role in many areas of chemistry, physics and materials science. The metal elements are able to form a large diversity of oxide compounds. In technological applications, oxides are used in the fabrication of microelectronic circuits, sensors, piezoelectric devices and fuel cells, coatings for the passivation of surfaces against corrosion and as catalysts [6-9]. One of the most promising materials in this regard is tin dioxide (SnO<sub>2</sub>). Semiconducting tin oxide thin films with suitable catalysts in the form of nanoparticles, overlayers, clusters etc. are known to exhibit enhanced sensitivity, better selectivity and fast response speeds to various reducing gases. SnO<sub>2</sub> sensors are invariably anion deficient and oxygen vacancies are mainly responsible for making available free electrons for the conduction process. In addition, the surface morphology of the sensing layer is also important for realization of sensor with enhanced

response characteristics, which in turn depend on the growth kinetics [10, 11].

SnO<sub>2</sub> films have a wide range of applications because of their excellent performance along with high mechanical, chemical and environmental stability and low cost material [12, 13]. By volume, the most deposited transparent conductive oxide (TCO) today is SnO<sub>2</sub>, which is used in IR-efficient architectural window application. In addition, it is receiving more attention for photovoltaic devices, especially for the heterojunction with intrinsic thin layer cells and related cells Si [14]. Another major application of intrinsic tin oxide is using it as gas sensors [15, 16]. Doped tin oxide, especially fluorine doped tin oxide, can be used as an ideal TCO layer in different applications such as transparent electrode in the solar cells. SnO<sub>2</sub> is a special oxide material because it has a low electrical resistance with high optical transparency in the visible range. Due to these properties, apart from gas sensors, SnO<sub>2</sub> is being used in many other applications, such as electrode materials in solar cells, light-emitting diodes, flat-panel displays and other optoelectronic devices where an electric contact needs to be made without obstructing photons from either entering or escaping the optical active area and in transparent electronics, such as transparent field effect transistors [17]. SnO<sub>2</sub> owing to a wide bandgap is an insulator in its stoichiometric form. However, due to the high intrinsic defects, that are oxygen deficiencies, tin oxide possesses a high conductivity. It has been shown that the formation energy of oxygen vacancies and tin interstitials in SnO<sub>2</sub> is very low. Therefore, these defects

form readily, which explains the high conductivity of pure, but nonstoichiometric, tin oxide [18, 19].

SnO<sub>2</sub> thin films have been deposited using different techniques, such as spray pyrolysis [20], sol-gel process [21], chemical vapour deposition [22], sputtering [23] and pulsed laser deposition [24]. Rao et al. successfully explained transition metal oxides with diverse structures, properties and phenomena have been the focus of much attention in recent years in view of their scientific and technological applications. These transition metal oxides, exhibit interesting structural, chemical, electrical and optical properties [25-28]. Ravindranadh et al. successfully prepared Co<sup>2+</sup> doped SnO<sub>2</sub> thin films and the crystal system is indexed to tetragonal rutile phase. PL spectrum of prepared samples shows strong yellow emission with suppressed blue emission and these materials are useful for display and LED devices [29]. Among these, spray pyrolysis is the most convenient method because of its simplicity, low cost, easy to add doping materials and the possibility of varying the film properties by changing composition of starting solution. In the present work, Fe<sup>3+</sup> doped (0.01 mol %) SnO<sub>2</sub> thin films were prepared by using chemical spray pyrolysis method. The prepared thin films were characterized by FT-IR, SEM with EDS, TEM and PL studies to collect the information about the luminescent properties of the prepared sample.

## 2. Experimental

All the chemicals used in the work were of analytical grade. Fe<sup>3+</sup> doped SnO<sub>2</sub> thin films were prepared by chemical spray pyrolysis. Spray solution was prepared by mixing 0.1 M aqueous solutions of SnO<sub>2</sub> and Fe<sub>2</sub>O<sub>3</sub> (0.01 mol %) using magnetic stirrer. The automated spray solution was then transferred to the hot substrate kept at the normalized deposition temperature of 673 K using filtered air as carrier gas at a flow rate normalized to approximately 1.8 ml/min. To prevent the substrate from excessively cooling, the prepared solution was sprayed on the substrate for 10 s with 15 s intervals. The films deposited onto micro-glass slides were first cleaned with detergent water and then dipped in acetone. Scanning electron microscope (SEM) and energy dispersive spectrum (EDS) images are taken on ZEISS EVO 18. Transmission electron microscope (TEM) images are recorded on HITACHI H-7600 and CCD CAMERA system AMTV-600 by dispersing samples in ethanol. Bruker FT-IR spectrophotometer is used for recording FT-IR spectrum of the prepared samples in the region 400-4000 cm<sup>-1</sup>. Photoluminescence (PL) spectrum is taken at room temperature on Horiba Jobin-Yvon Fluorolog-3 spectrofluorimeter with Xe continuous (450 W) and pulsed (35 W) lamps as excitation sources.

## 3. Results and discussion

Fe<sup>3+</sup> doped (0.01 mol %) SnO<sub>2</sub> thin films were prepared by using chemical spray pyrolysis method. The prepared thin films were characterized by FT-IR, SEM with EDS, TEM and PL studies to collect the information

about the luminescent properties of the prepared sample. The analysis of X-ray diffraction pattern revealed that the prepared tin oxide films are pure crystalline in nature.

### 3.1. Morphological studies

The morphology and chemical composition of as synthesized thin film was investigated by SEM and EDS analysis. Fig. 1 shows the SEM micrographs of Fe<sup>3+</sup> doped SnO<sub>2</sub> thin films taken with different magnifications. It can be clearly observed from low resolution SEM images that, the prepared sample show many agglomerates with an irregular morphology. The agglomeration could be induced by densification resulting from the narrow space between particles. SEM images reveal that the sample consists of irregular shaped sphere like structures. The incorporation of iron into the host material was confirmed by EDS measurements. The observed EDS pattern was shown in Fig. 2. The pattern showed the elemental compositions of Sn, O and iron. From this it was confirmed that the prepared sample contains doped iron species. TEM measurements were performed to confirm the nanocrystalline nature of the samples and to study the morphology of the particles. The TEM images of Fe<sup>3+</sup> doped SnO<sub>2</sub> thin films are depicted in Fig. 3. The particles are more or less uniformed in size and of irregular shape [30].

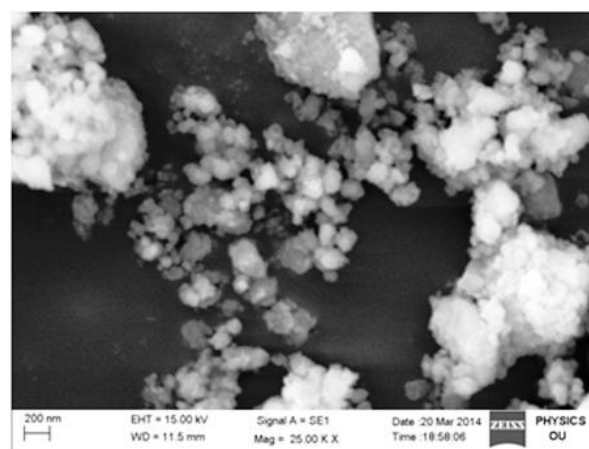


Fig. 1. SEM image of Fe<sup>3+</sup> doped SnO<sub>2</sub> thin films

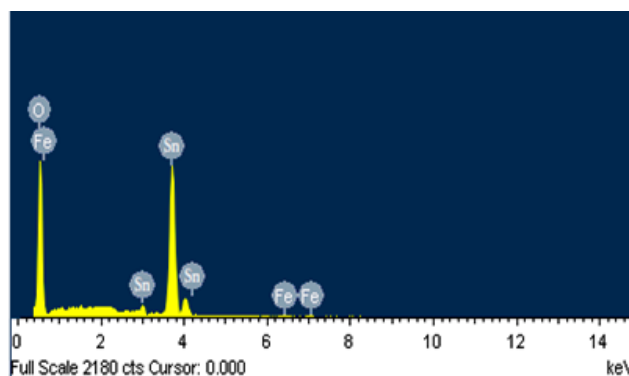


Fig. 2. EDS spectrum of Fe<sup>3+</sup> doped SnO<sub>2</sub> thin films

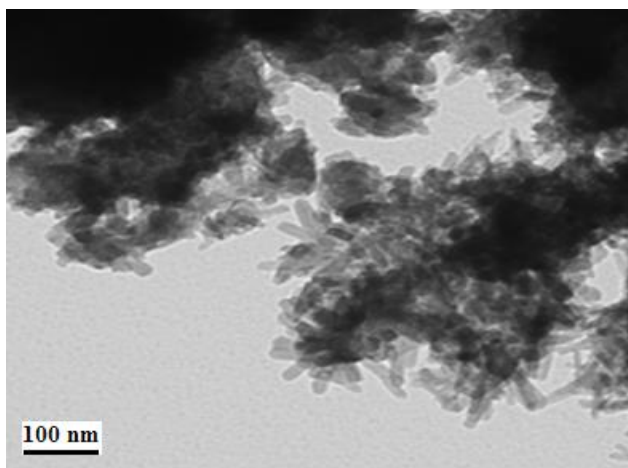


Fig. 3. TEM image of  $\text{Fe}^{3+}$  doped  $\text{SnO}_2$  thin films

### 3.2. FT-IR studies

FT-IR spectrometry was used for the determination of existing surface species. The FT-IR spectrum of  $\text{Fe}^{3+}$  doped  $\text{SnO}_2$  thin films was illustrated in Fig. 4. The bands at the low wavenumbers ( $500\text{--}1000\text{ cm}^{-1}$ ) could be attributed to  $\text{SnO}_2$ . The peaks at  $677$ ,  $786$  and  $965\text{ cm}^{-1}$  were assigned to O–Sn–O, Sn–O–Sn stretching vibrations and lattice vibrations, while the peaks at  $569$  and  $864\text{ cm}^{-1}$  were due to Sn–OH bonds of the  $\text{SnO}_2$  crystalline phase [31]. The bands observed in the region  $2500\text{--}1640\text{ cm}^{-1}$  are due to symmetric and asymmetric vibrations of hydroxyl ions situated at different sites in the lattice.

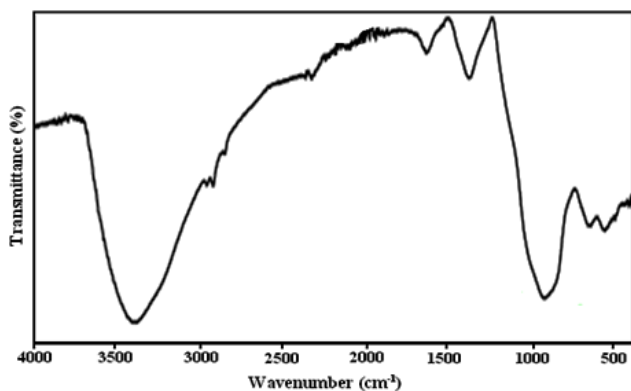


Fig. 4. FT-IR spectrum of  $\text{Fe}^{3+}$  doped  $\text{SnO}_2$  thin films

### 3.3. Photoluminescence studies

Fig. 5 shows the room temperature PL spectrum of  $\text{Fe}^{3+}$  doped  $\text{SnO}_2$  thin films under the excitation wavelength of  $280\text{ nm}$ . The spectrum exhibits two emission bands: a strong UV emission band at  $374\text{ nm}$  and a weak blue emission band at  $452\text{ nm}$ .

The emission bands of  $\text{Fe}^{3+}$  doped  $\text{SnO}_2$  thin films  $374$  and  $452\text{ nm}$  are assigned to the transition  ${}^4\text{T}_{2g}(\text{D}) \rightarrow {}^6\text{A}_{1g}(\text{S})$  and  ${}^4\text{A}_{1g}(\text{G}) \rightarrow {}^6\text{A}_{1g}(\text{S})$  [32]. The emission

spectrum of  $\text{Fe}^{3+}$  doped  $\text{SnO}_2$  thin films exhibits near band edge (NBE) emission in UV region and the deep level emission in visible regions [33]. By doping  $\text{Fe}^{3+}$  in  $\text{SnO}_2$  the emission bands are blue shifted and the quenching of visible luminescence and enhancement of UV emission was observed. The strong UV emission is observed for materials with better crystal quality [34]. In this study, a sharp and dominated UV emission at  $374\text{ nm}$  and a suppressed blue emission at  $452\text{ nm}$  in  $\text{Fe}^{3+}$  doped  $\text{SnO}_2$  thin films indicate that the prepared samples have better crystal quality and good optical properties with less defect states [35].

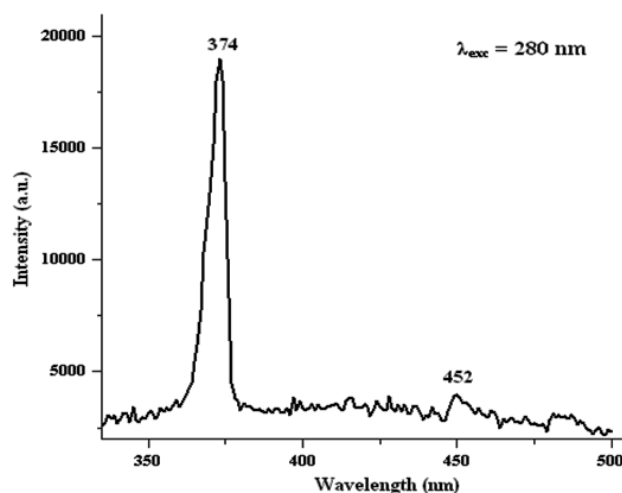


Fig. 5. PL spectrum of  $\text{Fe}^{3+}$  doped  $\text{SnO}_2$  thin films

### 3.4. Chromaticity properties

Most lighting specifications refer to colour in terms of the Commission Internationale de l'Éclairage (CIE) 1931 chromatic colour coordinates which recognize that the human visual system uses three primary colours: red, green and blue [36]. In general, the colour of any light source can be represented on the  $(x, y)$  coordinate in colour space. Colour purity was compared to the 1931 CIE Standard Source C (illuminant Cs). The chromatic coordinates  $(x, y)$  was calculated using the CIE coordinate calculator. The CIE chromaticity coordinates of  $\text{Fe}^{3+}$  doped  $\text{SnO}_2$  thin films were calculated from the emission spectrum. The location of the colour coordinates for  $\text{Fe}^{3+}$  doped  $\text{SnO}_2$  thin films in the CIE chromaticity diagram is shown in Fig. 6 by a solid circle sign ( $\bullet$ ). From this figure, one can see that the colour of  $\text{Fe}^{3+}$  doped  $\text{SnO}_2$  thin films located in the blue region and the CIE coordinates are  $(x = 0.145, y = 0.116)$ . These characteristic features may represent the possible applications in the fields of UV back lights, UV LEDs and display devices.

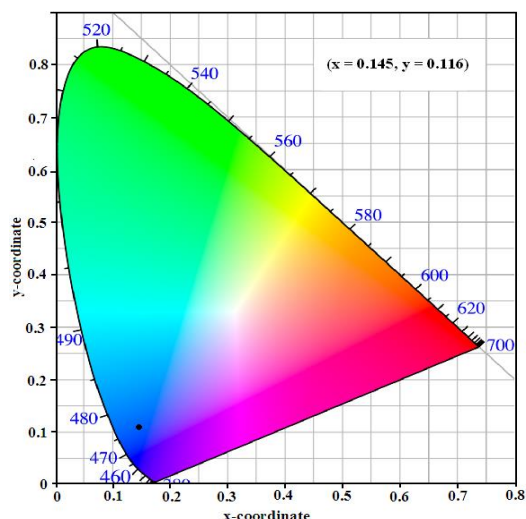


Fig. 6. CIE diagram of Fe<sup>3+</sup> doped SnO<sub>2</sub> thin films

#### 4. Conclusion

Fe<sup>3+</sup> doped SnO<sub>2</sub> thin films were prepared successfully by chemical spray pyrolysis method. SEM micrographs shows irregular shaped sphere like structures and EDS analysis confirms the presence of constituent elements of the prepared material. TEM images clearly show the formation of nano rods. FT-IR spectrum showed the characteristic vibrational modes of host lattice. PL spectrum of Fe<sup>3+</sup> doped SnO<sub>2</sub> thin films shows strong UV emission with suppressed blue emission. From CIE diagram, Fe<sup>3+</sup> doped SnO<sub>2</sub> thin films emits blue colour light and the corresponding coordinates are (x = 0.145, y = 0.116) and these materials may be useful for UV and display devices.

#### References

- [1] K. L. Chopra, S. Major, D. K. Pandya, Thin Solid Films **102**(1), 1 (1983).
- [2] J. Kennedy, P. P. Murmu, J. Leveneur, A. Markwitz, J. Futter, Appl. Surf. Sci. **367**, 52 (2016).
- [3] J. Kennedy, A. Markwitz, Z. Li, W. Gao, C. Kendrick, S. M. Durbin, R. Reeves, Cur. Appl. Phys. **6**(3), 495 (2006).
- [4] P. P. Murmu, J. Kennedy, Inter. J. Chem. Tech. Res. **7**(3), 1651 (2015).
- [5] J. Kennedy, B. Sundrakannan, R. S. Katiyar, A. Markwitz, Z. Li, W. Gao, Cur. Appl. Phys. **8**(3-4), 291 (2008).
- [6] M. C. Rao, Int. J. Chem. Sci. **10**(2), 1111 (2012).
- [7] M. C. Rao, Optoelectron. Adv. Mat. **6**(3-4), 511 (2012).
- [8] M. C. Rao, O. M. Hussain, Ind. J. Eng. Mater. Sci. **16**(5), 335 (2009).
- [9] M. C. Rao, O. M. Hussain, Res. J. Chem. Sci. **1**(7), 92 (2011).
- [10] H. Hosono, Thin Solid Films **515**(15), 6000 (2007).
- [11] K. Ravindranadh, D. Sridhar Kumar, K. Durga Venkata Prasad, M. C. Rao, Inter. J. Chem. Tech. Res. **9**(4), 598 (2016).
- [12] C. G. Granqvist, Thin Solid Films **515**, 7025 (2007).
- [13] H. L. Hartnagel, A. L. Dawar, A. K. Jain, C. Jagadish, Semiconducting Transparent Thin Films, IOP Publ. Ltd., London (1995).
- [14] E. Fortunato, D. Ginly, H. Hosono, D. C. Paine, MRS Bull. **32**(3), 242 (2007).
- [15] J. W. Bae, S. W. Lee, G. Y. Yeom, J. Electrochem. Soc. **154**(1), D34 (2007).
- [16] M. R. Vaezi, S. K. Sadrnezhad, Mater. Sci. Eng. B **140**(1-2), 73 (2007).
- [17] J. F. Wager, Science **300**(5623), 1245 (2003).
- [18] R. L. Hoffman, B. J. Norris, J. F. Wager, Appl. Phys. Lett. **82**(5), 733 (2003).
- [19] M. C. Rao, K. Ravindranadh, T. Satyanarayana, Y. Dasaradhu, G. Nagarjuna, K. Srinivas, M. S. Shekhawat, Der Pharma Chem. **8**, 243 (2016).
- [20] S. D. Shinde, G. E. Patil, D. D. Kajale, V. B. Gaikwad, G. H. Jain, J. Alloys Compd. **528**, 109 (2012).
- [21] C. Cobianu, C. Savaniu, P. Siciliano, S. Capone, M. Utriainen, L. Niinisto, Sens. Actuators B **77**(1-2), 496 (2001).
- [22] R. Larciprete, E. Borsella, P. De Padova, P. Perfetti, G. Faglia, G. Sberveglieri, Thin Solid Films **323**(1-2), 291 (1998).
- [23] G. Sberveglieri, G. Faglia, S. Gropelli, P. Nelli, Sens. Actuators B **8**(1), 79 (1992).
- [24] R. Dolbec, M. A. El Khakani, A. M. Serventi, R. G. Saint-Jacques, Sens. Actuators B **93**(1-3), 566 (2003).
- [25] M. C. Rao, AIP Conf. Proc. **1447**(1), 613 (2012).
- [26] M. C. Rao, J. Optoelectron. Adv. M. **12**(12), 2433 (2010).
- [27] M. C. Rao, AIP Conf. Proc. **1728**(1), 020077 (2016).
- [28] M. C. Rao, AIP Conf. Proc. **1536**, 27 (2013).
- [29] K. Ravindranadh, K. Durga Venkata Prasad, M. C. Rao, AIMS Mater. Sci. **3**, 796 (2016).
- [30] K. Kaviyarasu, Prem Anand Devarajan, S. Stanly John Xavier, S. Augustine Thomas, S. Selvakumar, J. Mater. Sci. Technol. **28**(1), 15 (2012).
- [31] A. F. Khan, M. Mehmood, M. Aslam, M. Ashraf, Appl. Surf. Sci. **256**(7), 2252 (2010).
- [32] K. Srinivasulu, I. Omkaram, H. Obeid, A. Suresh Kumar, J. L. Rao, J. Alloys Compd. **546**, 208 (2013).
- [33] S. L. Cho, J. Ma, Y. K. Kim, Y. Sun, G. K. L. Wong, J. B. Ketterson, Appl. Phys. Lett. **75**(18), 2761 (1999).
- [34] A. Umar, Y. B. Hahn, Nanotech. **17**(9), 2174 (2006).
- [35] H. Hao, M. Qin, P. Li, J. Alloys Compd. **515**, 143 (2012).
- [36] S. Shionoya, W. M. Yen, Phosphor Handbook, Phosphor Research Society, CRC Press, 459 (1998).

\*Corresponding author: raomc72@gmail.com